

Transition between self-focusing and self-defocusing in a nonlocally nonlinear system

Guo Liang,^{1,2} Weiyi Hong,¹ Tao Luo,¹ Jing Wang,¹ Yingbing Li,¹ Qi Guo,^{1,*} Wei Hu,¹ and Demetrios N. Christodoulides³

¹Guangdong Provincial Key Laboratory of Nanophotonic Functional Materials and Devices, South China Normal University, Guangzhou 510631, People's Republic of China

²School of Physics and Electrical Information, Shangqiu Normal University, Shangqiu 476000, People's Republic of China

³CREOL/College of Optics, University of Central Florida, Orlando, Florida 32816, USA



(Received 19 January 2019; published 5 June 2019)

We reveal the relevance between the nonlocality and the focusing and defocusing states in a nonlocally nonlinear system with a sine-oscillation response function, and predict a phenomenon that the self-focusing–self-defocusing property of the optical beam in the system depends on its degree of nonlocality. The transition from the focusing nonlinearity to the defocusing nonlinearity of the nonlinear refractive index will happen when the degree of nonlocality of the system goes across a critical value, and vice versa. We also discuss the bright soliton in the focusing state and the dark soliton in the defocusing state, respectively, for such a system.

DOI: [10.1103/PhysRevA.99.063808](https://doi.org/10.1103/PhysRevA.99.063808)

I. INTRODUCTION

The optical Kerr effect (OKE) [1–3], as one of the most important effects in nonlinear optics, is a fundamental and widespread phenomenon in the nonlinear interactions of light with materials, such as semiconductors [4], polymers [5], liquid crystals [6,7], soft matters [8], and photorefractive [9] and thermal [10–12] media. The equivalent OKE can also be found in optical quadratic nonlinear processes [13–15], and the other physical systems, such as Bose-Einstein condensates [16], quantum electron plasmas [17], and even on the surface of water [18]. The OKE refers to the light-intensity dependence of the refractive index n , that is, $n = n_0 + n_{nl}$, where n_0 is its linear part and n_{nl} is the light-induced nonlinear refractive index (NRI).

Optical solitons [3,19] are the main phenomena resulting from the OKE. The OKE is of two important intrinsic properties: the nonlocality and the focusing and defocusing. The NRI exhibits generally the nonlocality both in space and time [3]. In consideration of the spatial nonlocality in bulk materials, the NRI can be expressed phenomenologically as [3,20] $n_{nl} = n_2 \int_{-\infty}^{+\infty} R(x-x')|E(x',z)|^2 dx'$, where n_2 is the Kerr coefficient that is determined by material properties, the symmetric $R(x)$ is the response function of the media and E the optical field. For the local case, one has $n_{nl} = n_2|E|^2$ [1,2]; otherwise, the nonlocality is non-negligible. Systematic study on the nonlocality began with the work by Snyder and Mitchell [21]. Their work has attracted lots of attention [3,7,22–25], and experiments about the spatial nonlocality have been carried out in nematic liquid crystals [26], lead glasses [10], paraffin oils [11], and rhodamine aqueous solutions [12] for deeper and extensive investigations. On the other hand, the focusing and defocusing of the OKE refers to the phenomenon that the optical beam propagating in the bulk medium with the homogeneous n_0 can focus or defocus itself by its induced

NRI [1,2]. The material with $n_2 > 0$ or $n_2 < 0$ is called the self-focusing medium or the self-defocusing one, respectively [20]. It is commonly considered that the focusing-defocusing property is determined only by the medium properties, and has nothing to do with the nonlocality. In other words, the focusing and defocusing is irrelevant to the property of optical beams propagating in the medium.

In this paper, we will revisit the focusing-defocusing property of the media, and discover a dramatic relation between the focusing and defocusing and the nonlocality in the nonlocally nonlinear medium with a sine-oscillation response function, which was introduced in the study of quadratic solitons, obtained by Nikolov *et al.* [14] and then mentioned in the other works [15,27]. By defining the focusing and defocusing states, we have found that in such a system there exist the focusing and defocusing states, and their intertransition, which are related to the degree of nonlocality. Extensive discussions are also presented, including the bright and dark solitons in the focusing and defocusing states, respectively.

II. THEORETICAL MODEL

We consider the propagation of the optical beam along the z axis in a nonlocally nonlinear medium described by the system of equations for dimensionless complex optical field amplitude $\phi(x, z)$ and nonlinear refractive index $\Delta n(x, z)$ given by

$$i \frac{\partial \phi}{\partial z} + \frac{1}{2} \frac{\partial^2 \phi}{\partial x^2} + \Delta n \phi = 0, \quad (1a)$$

$$w_m^2 \frac{d^2 \Delta n}{dx^2} + s_n \Delta n - s |\phi|^2 = 0, \quad (1b)$$

where x and z stand, respectively, for the transverse and longitudinal coordinates scaled to a beam width and the Rayleigh distance, and w_m is the nonlinear characteristic length (NCL) of the system, and $s_n, s = \pm 1$. When $w_m = 0$ (the local case), the NRI $\Delta n = s_{tol} |\phi|^2$ with $s_{tol} = \text{sgn}(s_n s)$, and the system

*guoq@sncu.edu.cn

above is simplified into the well-known nonlinear Schrödinger equation $i\partial\phi/\partial z + (1/2)\partial^2\phi/\partial x^2 + s_{tol}|\phi|^2\phi = 0$, which has the stable sech-form bright soliton for $s_{tol} = 1$ and the stable tanh-form dark soliton for $s_{tol} = -1$, respectively [3,31]. When $w_m \neq 0$, the model given by Eqs. (1) with $s_n = s = -1$ can govern the interaction between an optical beam and the nematic liquid crystal with reorientational nonlocal nonlinearity [6,7]. If the term $|\phi|^2$ is replaced by ϕ^2 in Eq. (1b), the model (1) with $s_n = \pm s = \pm 1$ can also describe the parametric process between a fundamental wave and its second harmonic in quadratic nonlinear materials [14,15,27]. In the paper, we assume that $s_n = 1$ and $s = \pm 1$, which can be deemed an extension of the two physical systems mentioned above, and discuss a boundary-value problem:

$$w_m^2 \frac{d^2 \Delta n}{dx^2} + \Delta n - s|\phi|^2 = 0, \quad (2a)$$

$$\Delta n|_{x=\pm l} = 0. \quad (2b)$$

To solve the boundary-value problem (2), first we obtain the general solution of Eq. (2a), $\Delta n(x) = C \cos(x/w_m) + D \sin(x/w_m) + \Delta n_2(x)$, where $\Delta n_2(x) = (s/w_m) \int_{-l}^x |\phi(\xi)|^2 \sin[(x-\xi)/w_m] d\xi$ is its special solution, which can be obtained by the method of variation of parameters. Two constants C and D are determined by boundary condition given by Eq. (2b), i.e., $C \cos(l/w_m) + D \sin(l/w_m) = -\Delta n_2(l)$ and $C \cos(l/w_m) - D \sin(l/w_m) = 0$. Depending on its coefficient determinant, $\sin(2l/w_m)$, the solutions to boundary-value problem (2) exhibit two forms:

Case 1. When $\sin(2l/w_m) \neq 0$ (the case discussed in Ref. [27]), we have

$$C = -\frac{\Delta n_2(l)}{2 \cos(l/w_m)}, \quad D = -\frac{\Delta n_2(l)}{2 \sin(l/w_m)}. \quad (3)$$

Then $\Delta n(x) = s \int_{-l}^l R(x, \xi) |\phi(\xi)|^2 d\xi$, and the response function R is not of the translation invariance

$$R(x, \xi) = \begin{cases} -\frac{\sin\left(\frac{l+\xi}{w_m}\right) \sin\left(\frac{l-x}{w_m}\right)}{w_m \sin\left(\frac{2l}{w_m}\right)}, & \xi \leq x, \\ -\frac{\sin\left(\frac{l-\xi}{w_m}\right) \sin\left(\frac{l+x}{w_m}\right)}{w_m \sin\left(\frac{2l}{w_m}\right)}, & \xi \geq x, \end{cases} \quad (4)$$

which is the same as that in Ref. [27] when $l_1 = -l$ and $l_2 = l$.

Case 2. The case that $\sin(2l/w_m) = 0$ (i.e., $l = m\pi w_m/2$ with m an integer) can be decomposed into two situations: $\sin(l/w_m) = 0$ and $\cos(l/w_m) = 0$. In the former situation solutions exist only for even function $|\phi|^2$, and we have $C = 0$ and can determine D by taking the limit of Eq. (3) as $l \rightarrow m\pi w_m$. Similar treatments are for the latter situation, and solutions exist only for odd function $|\phi|^2$. For the two situations, the solution can be uniformly expressed by $\Delta n(x) = s \int_{-l}^l R(x-\xi) |\phi(\xi)|^2 d\xi$, and now the response function has the translation invariance

$$R(x) = \frac{1}{2w_m} \sin\left(\frac{|x|}{w_m}\right). \quad (5)$$

However, the optical intensity $|\phi|^2$ is considered to be of even symmetry; the second situation cannot exist here. Further, if l (equivalent m) is large enough so that $l \gg \max(w_m, w)$,

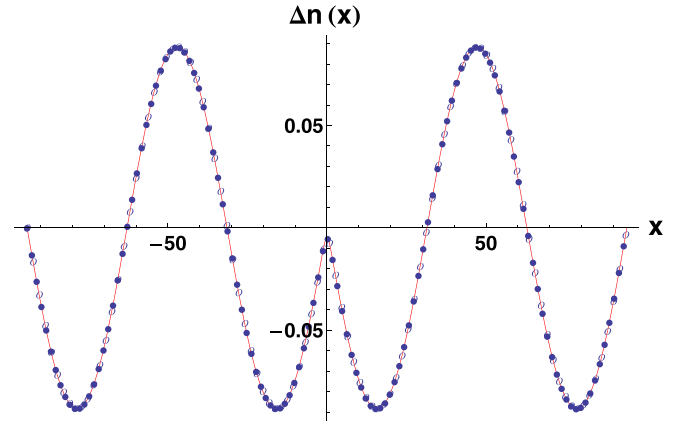


FIG. 1. Profiles of $\Delta n(x)$. Solid red curve is obtained by directly solving the boundary-value problem (2) with $l = 30\pi$; empty and filled circles are obtained by Eq. (6), and the calculation window is $[-30\pi, 30\pi]$ for the former, $[-300, 300]$ for the latter. We assume the Gaussian beam $\phi = \exp(-x^2/2)$, other parameters are $w_m = 10$ and $s = -1$.

$\Delta n(x)$ can be approximately expressed by a convolution

$$\Delta n(x, z) = s \int_{-\infty}^{\infty} R(x-x') |\phi(x', z)|^2 dx'. \quad (6)$$

In other words, when $l = m\pi w_m$ and $l \gg (w_m, w)$, the convolution (6) with response function $R(x)$ given by Eq. (5) is approximate to the solution of the boundary-value problem (2). The validity for our approximation can be readily proven, as shown in Fig. 1.

This kind of sine-oscillation response function given by Eq. (5) was obtained by Nikolov *et al.* [14], then extended to be discussed in other works [15,27]. The generalized degree of nonlocality (GDN) of the system is defined as $\sigma = w_m/w_r$, where the beamwidth $w_r = (2 \int_{-\infty}^{\infty} x^2 |\phi|^2 dx / \int_{-\infty}^{\infty} |\phi|^2 dx)^{1/2}$ [28], since the NCL w_m determines the oscillation period of $R(x)$ and does not represent any more the scale occupied by $R(x)$ like the case of the exponential-decay function [29].

III. FOCUSING-DEFOCUSING STATES AND THEIR INTER-TRANSITION

The nonlocal nonlinear system described by Eqs. (1a) and (6) exhibits focusing-defocusing states and their intertransition depending on the GDN, which will be shown in the following. To glimpse at the focusing-defocusing property of the nonlinear system, we simulate the propagation of an initial Gaussian beam with the input power P_0 ,

$$\phi_0(x) = \phi(x, z)|_{z=0} = \sqrt{\frac{P_0}{\sqrt{\pi} w_0}} \exp\left(-\frac{x^2}{2w_0^2}\right), \quad (7)$$

in Eqs. (1a) and (6), and show the typical results of the output beamwidth after propagating the distance $z = 1$ for the different initial GDN $\sigma_0 (= w_m/w_0)$ (the different w_0 and the fixed w_m) in Fig. 2(a). As can be observed in the figure, for a given P_0 , the output beamwidths will be larger or smaller, in the smaller or bigger sides of the σ coordinate respectively,

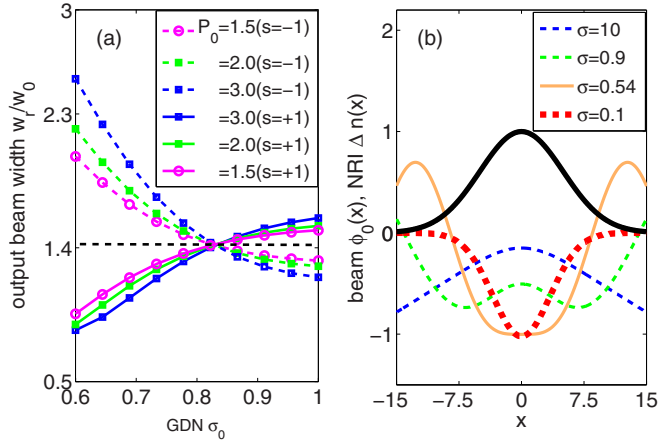


FIG. 2. (a) Normalized output beam widths w_r/w_0 at $z = 1$ (one Rayleigh distance) as the function of σ_0 , and the dashed black line presents the linear case where the analytic result is $w_r(z)/w_0 = \sqrt{1 + z^2}$ [30]. $w_m = 2$ for all of the curves. (b) Gaussian beam ϕ_0 (thick solid black line, $w_0 = 5$) and its induced NRI for different σ when $s = -1$. The NRI for $\sigma = 10$ is multiplied by 30.

than the linear case when $s = -1$; the inverse results will be obtained when $s = 1$. The higher the P_0 , the stronger the effect. It is well known that [1,2] the optical beam sampling the defocusing nonlinearity expands faster than that of the linear case; and the focusing case follows an opposite trend. Obviously, the focusing-defocusing nonlinearity sampled by the optical beams depends on its GDN σ dramatically for the nonlocal system described by Eqs. (1a) and (6). For the case that $s = -1$, the transition from the self-focusing to the self-defocusing will happen when σ goes down across the critical points $\sigma_c = 0.82$, which are the same and nothing to do with P_0 , and vice versa. The case that $s = +1$ is on the contrary.

The phenomenon observed above can be well understood through the relationship between the variations of the light intensity and its induced NRI distributions. We define the focusing-defocusing state of the NRI by the variation of the NRI distribution against that of the light intensity on the transverse perpendicular to the propagation direction z . The NRI has two states: focusing and defocusing. For the focusing state, the NRI changes uniformly with the intensity, that is, the NRI increases as the intensity increases, and vice versa; the defocusing state is on the contrary.

According to the definition, the focusing-defocusing states depend on the convexity and concavity of the NRI curves, and the sufficient condition for the realization of the transition between the focusing-defocusing states is that $d^2\Delta n/dx^2|_{x=0} = 0$.

For the local OKE [1,2] and the nonlocal OKE with nonoscillatory $R(x)$ [3,7,10,22,29], for example, the exponential-decay function [3,29], the focusing-defocusing states are only determined by $\text{sgn}(s)$ (the Kerr coefficient n_2 in the actual physical system). The focusing state appears when $s = 1$ ($n_2 > 0$), and the defocusing state does when $s = -1$ ($n_2 < 0$). The focusing-defocusing property of those two cases is determined only by the medium properties, and has nothing to do with the nonlocality, that is,

irrelevant to the property of optical beams propagating in the medium. No transition between them can happen in both cases because $d^2\Delta n/dx^2|_{x=0} \neq 0$. The system with a sine oscillation $R(x)$ given by Eq. (5), however, can realize the transition because $d^2\Delta n/dx^2|_{x=0} = 0$ for some critical points of the GDN. Since the NRI depends on the specific profile of the beams, by substituting the Gaussian beam (7) and the response function (5) into the NRI (6), after taking the second derivative with respect to x we obtain $d^2\Delta n/dx^2|_{x=0} = -sP_0[F(1/2\sigma) - \sigma]/\sqrt{\pi}w_m^3$, where $F(x) = \exp(-x^2)\int_0^x \exp(t^2)dt$ is the Dawson function, and a critical GDN $\sigma_{cg} = 0.54$. Figure 2(b) shows the transition process for $s = -1$ by giving the different curves of the NRI for different σ . For smaller σ such that $\sigma < \sigma_{cg}$, the NRI is defocusing, and the beam samples the defocusing index, then will be self-defocused, as can be observed in Fig. 2(a). When σ exceeds σ_{cg} , the focusing state of the NRI appears in the center, and both the range and the amplitude of the bell-shaped NRI increases as σ increases. When σ is slightly larger than σ_{cg} , moreover, the NRI is partially focusing and partially defocusing such that the central part of the beam samples the focusing index and its edges “see” the defocusing one. The optical beam as a whole will continue to exhibit the self-defocusing behavior until the effect of the focusing-index dominates.

This can explain why σ_{cg} is smaller than the critical points $\sigma_c = 0.82$ in Fig. 2(a). The exact inverse is the case that $s = 1$. The transition from the self-focusing to self-defocusing of the optical beam will happen when the GDN σ_0 goes up across a critical value. Figure 3 shows the evolutions of the Gaussian beam (7) for different values of σ in the two cases of $s = 1$ and $s = -1$, where the GDN dependent focusing and defocusing effects can be obviously observed.

IV. SOLITONS AND THEIR STABILITIES

Bright and dark solitons may exist when the optical beams sample the focusing and defocusing index, respectively [19,31]. Since the self-focusing–self-defocusing property of the system of Eqs. (1a) and (6) depends on its degree of nonlocality, then it will be readily expected that both bright and dark solitons can exist in different sides of the GDN σ for this system, which will be discussed respectively for situations that $s = -1$ and $s = 1$.

In higher range of GDN σ ($\sigma > \sigma_c$) for the case that $s = -1$, optical beams sample the focusing index, and bright solitons can form, while dark solitons may exist in the defocusing side of σ ($\sigma < \sigma_c$).

By the imaginary-time method [32], the numerical soliton solutions, $\phi = u(x)\exp(i\lambda z)$, of Eqs. (1a) plus (6) are obtained in the range $\sigma > \sigma_{bsc}$ ($\sigma_{bsc} = 1.21$)! No soliton solutions can be found in the lower range that $\sigma < \sigma_{bsc}$. Shown in Figs. 4 are the σ spectrums of the critical power of the soliton $P_c (= \int u^2 dx)$ and the soliton propagation constant λ (that is, the dependencies of P_c and λ upon σ). The bright solitons of the system described by Eqs. (1a) and (5) with $s = -1$ have two abnormal properties. First, the soliton propagation constants λ are negative, which results from the negative $\Delta n(x)$ [34]. For the bright solitons obtained before in the local nonlinear media [3,19] and the nonlocally nonlinear media with the

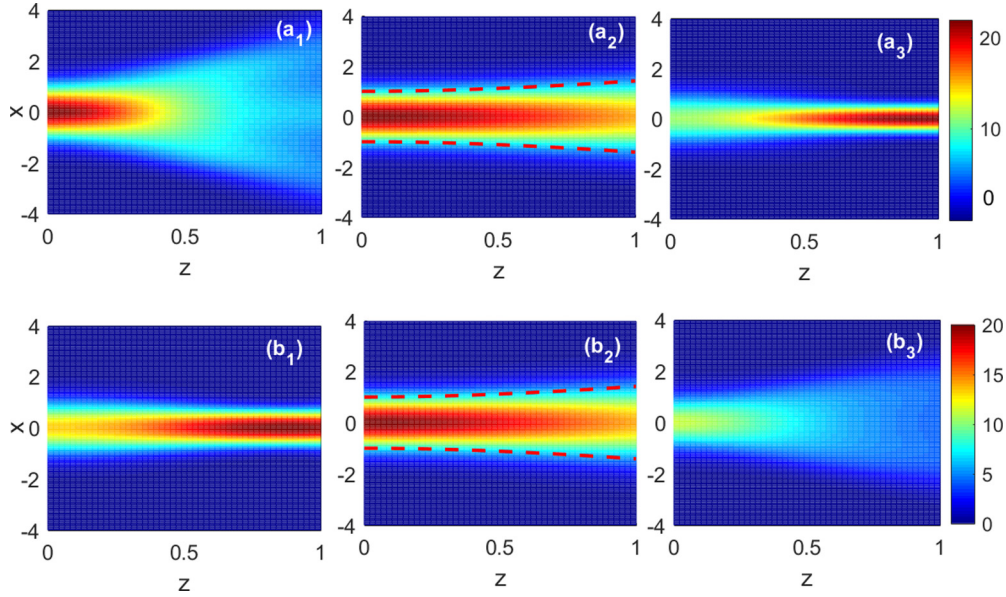


FIG. 3. Evolutions of Gaussian beams for both $s = -1$ (a1, a3) and $s = 1$ (b1, b3). $\sigma_0 = 0.45$ in (a1) and (b1), whereas $\sigma_0 = 1.2$ in (a3) and (b3). The linear evolutions are displayed in (a2) and (b2) for comparison.

nonoscillatory response function [3,7,22–25,35,36], however, their propagation constants are all positive. Second, the slope of the $P_c(\lambda)$ is negative, as shown in Fig. 4. Therefore, their stability criterion obeys an inverted Vakhitov-Kolokolov stability criterion [37]. The solitons obtained above are localized modes of the NRI waveguide but not the leaky modes presented in Ref. [38]. The propagation constants of the solitons obtained by us here are all real, as shown in Fig. 4, while those of the leaky modes are complex (imaginary parts account for radiation) [38].

To elucidate the linear stability of bright solitons, as done by Xu *et al.* in Ref. [39], we searched for perturbed solutions in the form $\phi(x, z) = [u(x) + \mu(x, z) + iv(x, z)] \exp(i\lambda z)$, where perturbations μ and v can grow with a complex rate δ on propagation. Linearization of Eq. (1a) around $u(x)$ yields

the following system of equations:

$$\delta\mu = -\frac{1}{2} \frac{d^2 v}{dx^2} + \lambda v - \mu v, \tag{8}$$

$$\delta v = \frac{1}{2} \frac{d^2 \mu}{dx^2} - \lambda \mu + \mu v + u \Delta N, \tag{9}$$

where $\Delta N = -2 \int_{-\infty}^{\infty} R(x-x')u(x')\mu(x')dx'$ is the refractive-index perturbation. We have solved the system of Eqs. (8) and (9). The result of the stability analysis summarized in Table I shows that all the solitons, if found numerically, are stable, which is also confirmed by the simulations, as shown in Figs. 5(c) and 5(d).

In the defocusing side of σ ($\sigma < \sigma_c$) for $s = -1$, the optical beam samples the defocusing index. The exact dark soliton solution was found to exist in the condition that $w_m/w_0 \leq 1/2$ [40], $|\phi(\xi)| = \frac{\sqrt{2}w_m}{2w_0} \sqrt{36 \tanh^4(\xi) + (\frac{6w_0^2}{w_m^2} - 48) \tanh^2(\xi) + 4 - \frac{(4w_m^2/w_0^2 - 1)}{w_m^4/w_0^4}}$ with $\xi = (x - vz)/w_0$, where the parameter v denotes the tangent of an incident angle of the dark soliton, and can be assumed that $v = 0$ in the normal incidence case. By defining the width of the dark soliton as $w_r = [2 \int_{-\infty}^{+\infty} x^2 (|\phi_\infty|^2 - |\phi|^2) dx / \int_{-\infty}^{+\infty} (|\phi_\infty|^2 - |\phi|^2) dx]^{1/2}$ with $|\phi_\infty|$ being the background amplitude, we have its GND $\sigma = (\sqrt{2}w_m/w_0) / \sqrt{\pi^2/3 + 8(w_m/w_0)^2}$, and then find that the σ range for the existence of the dark soliton is

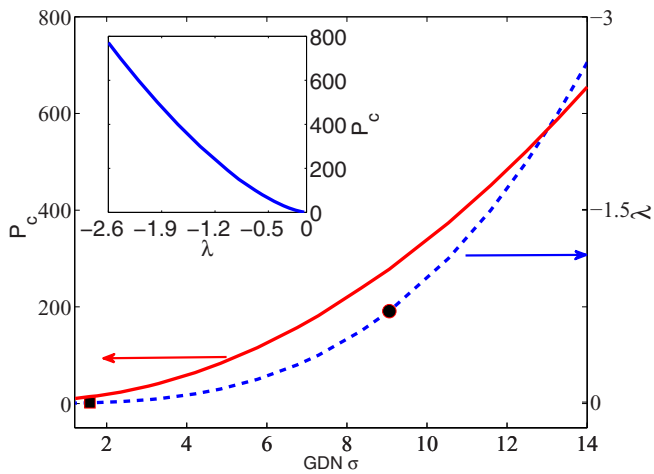


FIG. 4. Critical power P_c and the soliton propagation constant λ vs the GDN σ . The inset shows P_c vs λ . All of the results are obtained for $w_m = 10$.

TABLE I. Real part of the perturbation growth rate δ for the bright solitons vs the generalized degree of nonlocality σ .

σ	10.534	9.236	8.352	7.287	5.763
$\text{Re}(\delta) (\times 10^{-13})$	3.550	3.979	5.462	4.463	3.973
σ	4.208	3.298	2.351	1.761	1.212
$\text{Re}(\delta) (\times 10^{-13})$	2.341	5.115	2.842	4.545	8.530

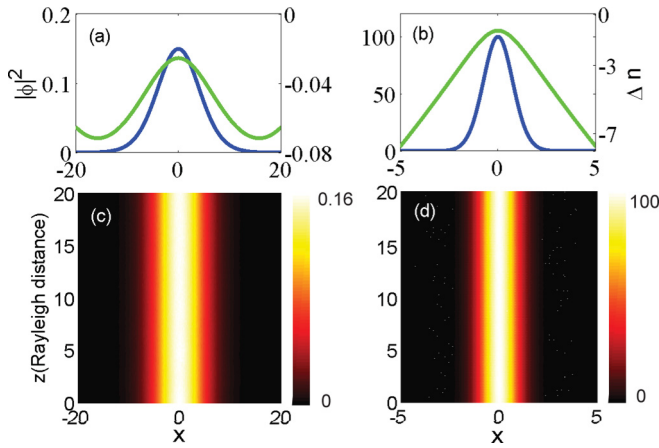


FIG. 5. The solitons (solid blue lines) for the small $\sigma(=1.58)$ (a) and the large $\sigma(=9.06)$ (b), which correspond, respectively, to the filled square and the filled circle in Fig. 4, and solid green lines represent the corresponding NRI. The numerical propagations of the solitons with 5% random noises are shown in (c) and (d), respectively.

$\sigma \leq \sigma_{dsc}(=0.31)$. Modulation instability (MI) of system (1a) and (6) has been discussed, and the main result is that the MI always occurs [41]. Therefore, the dark soliton solutions are unstable when $w_m \neq 0$ due to the MI.

For the situation that $s = 1$, as discussed above, optical beams sample, respectively, the defocusing and focusing indexes in the higher and lower ranges of the GDN for such a situation. The case that $s = 1$ and the large GDN was discussed in Ref. [15], and no single-hump bright soliton was found, which is consistent with the phenomenon we discovered. When the boundary is involved, however, the single-hump bright soliton can sometimes exist for the case because the boundary can redistribute the NRI such that Δn can become focusing in the center region for some suitable conditions [27]. The dark solitons in the defocusing side ($\sigma > \sigma_c$), even if they exist, are unstable due to the existing MI [41]. Therefore, we only take the bright soliton in the focusing side ($\sigma < \sigma_c$) into consideration. Bright solitons with complicated structure were numerically found in the σ range of [0.28, 0.78], which were referred to as in-phase and out-of-phase bound-state solitons [42], among which the single-hump Gauss-like solitons did fall in the range $\sigma < \sigma_c$.

V. CONCLUSION

In conclusion, we have discussed the property of the nonlocally nonlinear system with the sine-oscillation response function [Eqs. (1a) and (6)], which is approximate to the model of Eqs. (1a) together with the boundary-value problem

σ -spectrum (range of the GDN σ)				
0				
0.31				
0.82(σ_c)				
1.21				
∞				
$s=-1$	unstable dark solitons	no	no	stable bright solitons
	defocusing nonlinearity		focusing nonlinearity	
$s=1$	focusing nonlinearity		defocusing nonlinearity	
	no	stable bright solitons	no	unknown
0				
0.28				
0.78				
0.82(σ_c)				
∞				

FIG. 6. σ spectrum of the defocusing and focusing states and the stability of the solitons.

(2) in the condition discussed in Sec. II, and found that its focusing-defocusing property depends on generalized degree of nonlocality of the system σ . The transition between defocusing and focusing states of the nonlinear refractive index will occur when σ goes across $\sigma_c(=0.82)$. In the case that $s = -1$, the bright and dark solitons exist, respectively, in the range that $\sigma > 1.21$ (the focusing side) and in the range that $\sigma < 0.31$ (the defocusing side) of the σ coordinate. The bright solitons are stable, and the dark solitons are unstable due to the existing MI. While for the case that $s = +1$, the single-hump Gauss-like bright solitons are in lower ranges of the GDN (the focusing side). The dark solitons in higher ranges of the GDN (the defocusing side), even if they exist, are also unstable due to the existing MI. In Fig. 6, we summarize the main results obtained so far for the nonlocal nonlinear system described by Eqs. (1a) and (6).

The model presented here is a reasonable extension of the two physical models that describe the reorientational nonlinearity in the nematic liquid crystal and the parametric process in the quadratic nonlinear material, respectively. A critic might question whether our model can be realized physically. Although it seems not so easy to find a medium whose nonlinear process can be described by the model so far, possibly our prediction would serve as an incentive for others to find natural materials or even metamaterials that could physically realize the interesting phenomenon found in this paper. As a matter of fact, the oscillation response function of the nonlocal nonlinearity was recently predicted for surface plasmon polaritons on a metal surface which hosts a thin film of a liquid dielectric [43].

ACKNOWLEDGMENT

This research was supported by the National Natural Science Foundation of China (Grants No. 11604199 and No. 11474109).

G. Liang and W. Hong have contributed equally to this work, with the first one mainly to analytical operations and the second one mainly to numerical simulations.

[1] Y. R. Shen, in *Principles of Nonlinear Optics* (Wiley, New York, 1984), p. 286.
 [2] R. W. Boyd, in *Nonlinear Optics*, 3rd ed. (Academic Press, Amsterdam, 2008), p. 207.
 [3] Q. Guo, D. Lu, and D. Deng, in *Advances in Nonlinear Optics*, edited by X. Chen, Q. Guo, W. She, H. Zeng, and G. Zhang (De Gruyter, Berlin, 2015), Chap. 4, pp. 227–305.

[4] M. Sheik-Bahae, D. J. Hagan, and E. W. Van Stryland, *Phys. Rev. Lett.* **65**, 96 (1990).
 [5] W. J. Blau, H. J. Byrne, D. J. Cardin, T. J. Dennis, J. P. Hare, H. W. Kroto, R. Taylor, and D. R. M. Walton, *Phys. Rev. Lett.* **67**, 1423 (1991).
 [6] C. Conti, M. Peccianti, and G. Assanto, *Phys. Rev. Lett.* **91**, 073901 (2003).

- [7] G. Assanto, *Nematicons: Spatial Optical Solitons in Nematic Liquid Crystals* (Wiley, New York, 2013).
- [8] C. Conti, G. Ruocco, and S. Trillo, *Phys. Rev. Lett.* **95**, 183902 (2005).
- [9] M. Segev, B. Crosignani, A. Yariv, and B. Fischer, *Phys. Rev. Lett.* **68**, 923 (1992).
- [10] C. Rotschild, O. Cohen, O. Manela, M. Segev, and T. Carmon, *Phys. Rev. Lett.* **95**, 213904 (2005).
- [11] A. Dreischuh, D. N. Neshev, D. E. Petersen, O. Bang, and W. Krolikowski, *Phys. Rev. Lett.* **96**, 043901 (2006).
- [12] N. Ghofraniha, C. Conti, G. Ruocco, and S. Trillo, *Phys. Rev. Lett.* **99**, 043903 (2007).
- [13] A. V. Buryak and Yu. S. Kivshar, *Phys. Lett. A* **197**, 407 (1995).
- [14] N. I. Nikolov, D. Neshev, O. Bang, and W. Z. Krolikowski, *Phys. Rev. E* **68**, 036614 (2003).
- [15] B. K. Esbensen, M. Bache, W. Krolikowski, and O. Bang, *Phys. Rev. A* **86**, 023849 (2012).
- [16] P. Pedri and L. Santos, *Phys. Rev. Lett.* **95**, 200404 (2005).
- [17] P. K. Shukla and B. Eliasson, *Phys. Rev. Lett.* **96**, 245001 (2006).
- [18] A. Chabchoub, O. Kimmoun, H. Branger, N. Hoffmann, D. Proment, M. Onorato, and N. Akhmediev, *Phys. Rev. Lett.* **110**, 124101 (2013).
- [19] Y. S. Kivshar and G. P. Agrawal, *Optical Solitons: From Fibers to Photonic Crystals* (Academic Press, New York, 2003).
- [20] Q. Guo, W. Hu, D. Deng, D. Lu, and S. Ouyang, in *Nematicons: Spatial Optical Solitons in Nematic Liquid Crystals*, edited by G. Assanto (Wiley, New York, 2013), Chap. 2, pp. 37–69.
- [21] A. W. Snyder and D. J. Mitchell, *Science* **276**, 1538 (1997).
- [22] W. Królikowski, O. Bang, N. I. Nikolov, D. Neshev, J. Wyller, J. J. Rasmussen, and D. Edmundson, *J. Opt. B: Quantum Semiclass. Opt.* **6**, S288 (2004).
- [23] M. Peccianti and G. Assanto, *Phys. Rep.* **516**, 147 (2012).
- [24] Q. Guo, *Proc. SPIE* **5281**, 581 (2003).
- [25] W. Królikowski, O. Bang, D. Briedis, A. Dreischuh, D. Edmundson, B. Luther-Davies, D. Neshev, N. Nikolov, D. E. Petersen, J. J. Rasmussen, and J. Wyller, *Proc. SPIE* **5949**, 59490B (2005).
- [26] C. Conti, M. Peccianti, and G. Assanto, *Phys. Rev. Lett.* **92**, 113902 (2004).
- [27] J. Wang, Y. Li, Q. Guo, and W. Hu, *Opt. Lett.* **39**, 405 (2014).
- [28] By this definition, the beamwidth w_r of the Gaussian beam $\phi_0(x)$ given by Eq. (7) is just equal to w_0 .
- [29] P. D. Rasmussen, O. Bang, and W. Królikowski, *Phys. Rev. E* **72**, 066611 (2005).
- [30] H. A. Haus, *Waves and Fields in Optoelectronics* (Prentice-Hall, Englewood Cliffs, NJ, 1984), pp. 109–111 and 159–160.
- [31] G. P. Agrawal, *Nonlinear Fiber Optics*, 3rd ed. (Academic Press, San Diego, 2001), Chap. 5, pp. 135–202.
- [32] M. L. Chiofalo, S. Succi, and M. P. Tosi, *Phys. Rev. E* **62**, 7438 (2000).
- [33] A. W. Snyder, S. J. Hewlett, and D. J. Mitchell, *Phys. Rev. Lett.* **72**, 1012 (1994).
- [34] Substitution of the soliton solution into Eq. (1a) yields $d^2u/dx^2 + 2[\Delta n(x) - \lambda]u = 0$. $u(x)$ can be considered as the localized mode of the self-induced waveguide $\Delta n(x)$ [33], and exists under the condition that $\lambda < \Delta n(x)$ at least in some range [30]. $\Delta n(0)$ can be easily proved to be negative, which is the maximum of $\Delta n(x)$ in the scope of the optical beam. Therefore, $\Delta n(x)$ is all negative in the scope, as observed in Figs. 2(b) and 5. Thus we have $\lambda < 0$.
- [35] Q. Guo, B. Luo, F. Yi, S. Chi, and Y. Xie, *Phys. Rev. E* **69**, 016602 (2004).
- [36] Q. Shou, X. Zhang, W. Hu, and Q. Guo, *Opt. Lett.* **36**, 4194 (2011).
- [37] H. Sakaguchi and B. A. Malomed, *Phys. Rev. A* **81**, 013624 (2010).
- [38] O. Peleg, Y. Plotnik, N. Moiseyev, O. Cohen, and M. Segev, *Phys. Rev. A* **80**, 041801(R) (2009).
- [39] Z. Xu, Y. Kartashov, and L. Torner, *Opt. Lett.* **30**, 3171 (2005).
- [40] Y. Hu and S. Lou, *Commun. Theor. Phys.* **64**, 665 (2015).
- [41] Z. Wang, Q. Guo, W. Hong, and W. Hu, *Opt. Commun.* **394**, 31 (2017).
- [42] G. Liang, W. Hong, and Q. Guo, *Opt. Express.* **24**, 28784 (2016).
- [43] S. Rubin and Y. Fainman, *Phys. Rev. Lett.* **120**, 243904 (2018).